

# Biaxial Shape Memory Effect Exhibited by Monodomain Chiral Smectic C Elastomers

Kazuyuki Hiraoka,<sup>\*,†</sup> Wataru Sagano,<sup>†</sup> Takuhei Nose,<sup>†</sup> and Heino Finkelmann<sup>\*</sup>

Center for Nano Science and Technology, Department of Nanochemistry, Tokyo Polytechnic University, 1583 Iiyama, Atsugi-shi 243-0297, Japan, and Institut für Makromolekulare Chemie, Albert-Ludwigs-Universität Freiburg, Stefan-Meier-Str. 31, D-79104 Freiburg i. Br., Germany

Received March 28, 2005; Revised Manuscript Received June 10, 2005

**ABSTRACT:** We show that a monodomain chiral smectic C elastomer exhibits a biaxial shape memory effect, demonstrating its spontaneous and reversible deformation in a heating and cooling process where successive phase transitions take place. Not only shrinkage (elongation) due to the smectic–isotropic (isotropic–smectic) transition but also spontaneous shear-deformation associated with molecular tilting in the smectic phases is observed. In addition, we discuss the relationship between the deformation of the monodomain elastomer and the local symmetry of liquid-crystalline phases by means of X-ray scattering observation.

## Introduction

Liquid-crystalline elastomers have been increasing attention as a novel class of liquid-crystalline materials because they give rise to new macroscopic features by combining the mechanical properties of polymer networks with the anisotropic structure of liquid-crystalline phases.<sup>1–7</sup> Over the past two decades, in particular, they have attracted both industrial and scientific interest because of their thermomechanical properties such as reversible strain actuation and soft elasticity.<sup>8–12</sup> Küpfer et al. reported that a uniformly aligned liquid-crystalline elastomer designated as a liquid single-crystal elastomer (LSCE) spontaneously and quickly elongates (shrinks) along its director during the phase transformation from an isotropic to a nematic phase.<sup>8</sup> Recently, Finkelmann et al.<sup>11</sup> and Tajbakhsh et al.<sup>12</sup> have reported that nematic elastomers containing liquid-crystalline main-chain polymers have the remarkable property of being able to change their shape by up to ~350–400% within a relatively narrow temperature interval straddling their nematic–isotropic (N–I) transition temperature,  $T_{ni}$ .

While there have been a few investigations on the reversible shape change of nematic elastomers, much less work has been carried out on those of smectic.<sup>13–17</sup> In particular there are few studies about the deformation of chiral smectic C (SmC\*) elastomers, despite their potential properties due to the point group  $C_2$  of the untwisted structure.<sup>18–29</sup> About a decade ago, Terentjev and Warner theoretically described the coupling between elastic deformation and the SmC order parameter for the limiting situation of small distortions.<sup>28,29</sup> These predictions have not been experimentally verified due to the lack of monodomain samples. Recently, we succeeded in obtaining these samples with macroscopic  $C_2$  symmetry of the unwound SmC\* state by two successive deformation processes<sup>30</sup> and more perfectly by mechanical shear deformation.<sup>31</sup> The purpose of this

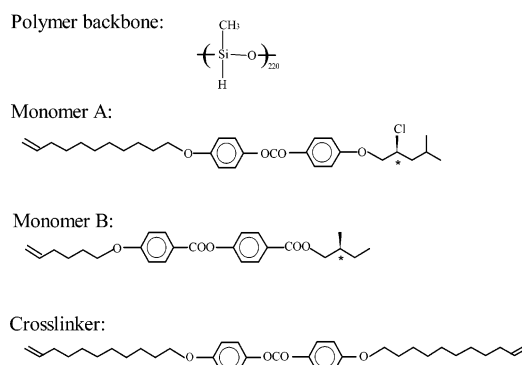


**Figure 1.** System under investigation.

paper is to show that the monodomain SmC\* elastomer obtained by a mechanical shear field exhibits a biaxial shape memory effect, which means spontaneous and reversible deformation occurs in a heating and cooling process where successive phase transitions take place. Not only shrinkage (elongation) due to the smectic–isotropic (isotropic–smectic) transition but also shear deformation associated with molecular tilting in the smectic phases is observed. In addition, we investigate the mechanism of the spontaneous and reversible deformations of the SmC\* elastomer by means of X-ray scattering observation. The X-ray analysis reveals that the macroscopic symmetry defined by the shape of the elastomer film corresponds to the local symmetry associated with the molecular alignment in the liquid-crystalline phase of the monodomain SmC\* elastomer.

## Experimental Section

**System.** An elastomer is synthesized by a hydro-silylation reaction of the liquid-crystalline side groups with a polysiloxane backbone according to the well-known synthesis route.<sup>1</sup> The chemical structures of the polymer backbone, the mesogens, and the cross linker are shown in Figure 1. The elastomer contains two different mesogenic moieties statistically linked to the monomer units of the network and shows the following phase sequence:

g – 6 SmX\* 32 SmC\* 80 SmA 115 I (in °C)

The SmX\*–SmC\* transition temperature is determined by differential scanning calorimetry (DSC) measurements. Since

\* To whom correspondence should be addressed. Tel.: +81-46-242-9526. Fax: +81-46-242-3000. E-mail: hiraoka@nano.t-kougei.ac.jp.

<sup>†</sup> Tokyo Polytechnic University.

<sup>‡</sup> Albert-Ludwigs-Universität Freiburg.

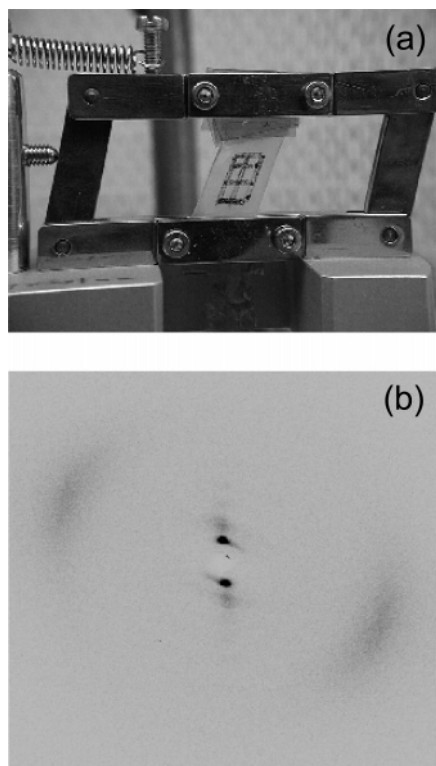


**Figure 2.** Sample preparation for monodomain SmC\* elastomer: (a) a photograph of an elastomer film fixed on the shear apparatus and (b) its X-ray diffraction pattern.

the SmC\*–SmA transition temperature  $T_{CA}$  is hardly confirmed in the DSC chart, it is tentatively determined at 80 °C on the basis of the temperature dependence of the molecular tilt angle calculated from the layer thickness estimated by X-ray measurements of uniaxially deformed elastomers; while the layer thickness increases with increasing temperature in the SmC\* phase up to  $T_{CA}$ , it remains almost constant on further increase of temperature.<sup>25,31,32</sup> In addition, the SmA–Iso transition temperature is also tentatively determined by the temperature dependence of the order parameter estimated by the X-ray measurements, because the DSC peak is very broad. While the X-ray pattern reveals that the SmX\* phase is one of the tilted smectic phases, the details will be published in another paper.

**Sample Preparation for Monodomain SmC\* Elastomer.**<sup>31</sup> The elastomer film is prepared by the spin-casting technique in solution, which contains the polysiloxane (2 mmol), mesogen A (1.2 mmol), mesogen B (0.4 mmol), the cross linker (0.2 mmol), and 6  $\mu$ L of the Pt catalyst SLM86005 (Wacker Chemie, Burghausen) in 2 mL of toluene. The reaction is carried out under centrifugation (3000 rpm) at 90 °C for 2 h. Thereafter, the reaction vessel is cooled to room temperature, and the elastomer, swollen with toluene, is carefully removed from the vessel. To obtain a uniform orientation of director, the swollen elastomer is deformed uniaxially by loading it with a stress of 25 mN/mm<sup>2</sup> for 1 h.

After the uniaxial deformation, the elastomer is fixed onto a simple shear apparatus and gradually sheared with an angle  $\theta$  of  $\sim 20^\circ$  at room temperature (25 °C), as shown in Figure 2a. The pattern painted on the film proves that the elastomer is deformed uniformly by the mechanical shear field. The elastomer is kept under mechanical shear field for about 3 h until the cross-linking reaction is completed. The isotropic solvent depresses the phase transformation, and if the concentration of the solvent decreases, the system passes the isotropic to liquid–crystal transformation. Namely, during these deformation processes at room temperature (25 °C), the toluene evaporates continuously from the network and the successive phase transformations occur from the isotropic phase of the gel to the tilted smectic phase of the dry network.

In addition, the sample is annealed within the SmC\* phase at 60 °C for about 1 h to accelerate the reorientation process. Finally a monodomain sample of the smectic C\* elastomer whose X-ray photograph is shown in Figure 2b was obtained.

**X-ray Measurements.** The alignment of the elastomer is observed by X-ray measurements with a rotating anode X-ray system. The measurements are mainly performed using a Cu K $\alpha$  beam filtered by a confocal mirror ( $\lambda = 1.54$  Å, X-ray power = 2.7 kW) and a two-dimensional image plate system (2540  $\times$  2540 pixels, 50  $\mu$ m resolution). The distance between the sample and image plate is 100 mm. The sample is mounted in a microfurnace, and the temperature-dependent X-ray measurements are carried out. Here, the sample hangs freely during the measurements so that the molecular alignments observed are not associated with any effect of externally applied strains.

## Results and Discussion

To investigate deformational behavior of the monodomain SmC\* elastomer during the successive phase transitions, the shape change of the elastomer film is observed in a cooling and heating process. A series of photographs of the monodomain SmC\* elastomer is shown in Figure 3, where the topside of the elastomer is fixed to a sample holder, while the lower end can move freely. While the shape of the elastomer is rhomboid at room temperature (Figure 3a), it transforms into a nearly rectangular-like shape in the temperature region of the SmA phase (Figure 3b). On further increase in temperature, the elastomer shrinks during the phase transition from the SmA phase to the isotropic phase (Figure 3c). It is noteworthy that the reverse deformation takes place in cooling from the isotropic to smectic phase. Namely, the elastomer spontaneously elongates during the Iso–SmA phase transition, and then the rectangular-like film (Figure 3d) transforms into a rhombic one (Figure 3e) on decreasing the temperature further into the smectic phase. In addition, it may be worth pointing out that the spontaneous distortion associated with the helical mechanoclinic effect, which has already been discussed theoretically,<sup>28,29</sup> is not confirmed in the present observation, because the cross-linking in the unwound SmC\* state prevents it. The experimental approach to the spontaneous distortion resulting from the Goldstone mode is a future problem.

To measure the elastomer's shape, the sample length  $L_E$  is defined as the distance between polyimide tapes. The tilt angle of the elastomer film  $\theta_E$  is defined as the angle between the edge of the film and the direction of the first uniaxial deformation, respectively (see parts a and c of Figure 3). To investigate the details of the shape change with varying temperature, both the sample length,  $L_E$ , and the tilt angle of elastomer,  $\theta_E$ , are plotted as a function of temperature in parts a and b of Figure 4, respectively. While  $L_E$  is about 8.0 mm at room temperature as shown in Figure 4a, it slightly increases with increasing temperature in the SmX\* and SmC\* phases. The value of  $L_E$  attains its maximum at about 8.5 mm in the SmA phase, and then it rapidly decreases to about 6.3 mm during the phase transformation from SmA to Iso. (Please note that the value estimated is likely not to be 100 percent accurate in the isotropic phase, as the elastomer buckles as seen in Figure 3c). One may notice that the value of ( $L_E/\cos \theta_E$ ) seems to be almost constant at about 8.7 mm. The reverse deformation is recognized on cooling, namely, the elastomer rapidly elongates from 6.3 to 8.5 mm at the phase transformation from Iso to SmA and then  $L_E$  decreases

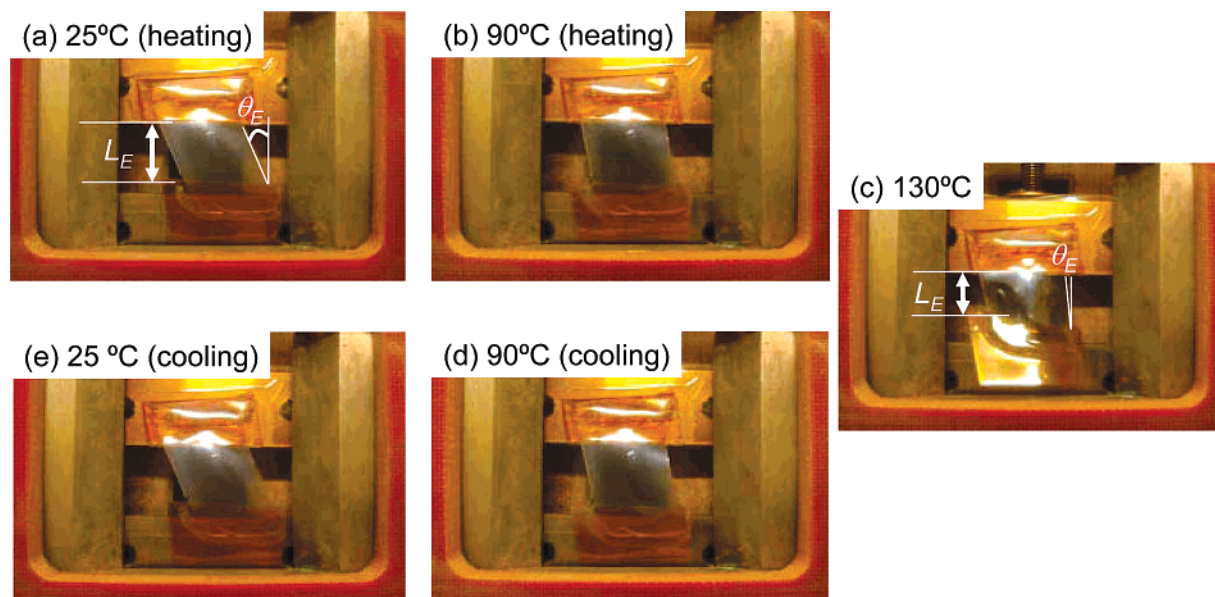


**Figure 3.** Photographs of a monodomain SmC\* elastomer in a heating and cooling process. The topside of the elastomer was fixed to a sample holder, while the lower end could freely move.

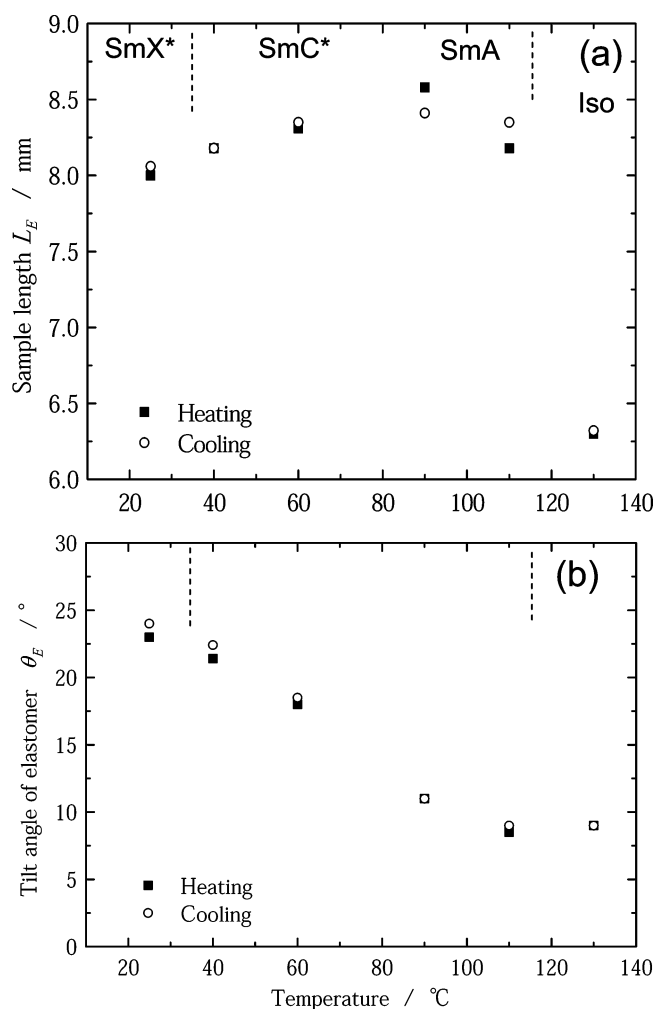


**Figure 4.** Temperature dependences of (a) sample length  $L_E$  and (b) tilt angle  $\theta_E$  of an elastomer film.

slightly with decreasing temperature in the SmC\* and SmX\* phases.

The temperature dependence of the tilt angle  $\theta_E$  of the elastomer is shown in Figure 4b.  $\theta_E$ , which is about 23° at room temperature, decreases with increasing

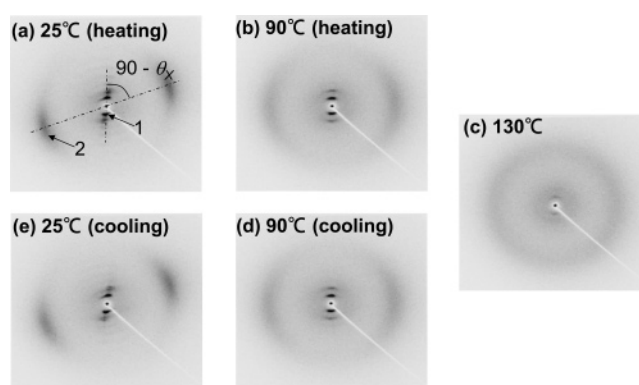


**Figure 5.** X-ray patterns of a monodomain SmC\* elastomer in a heating and cooling process. Here, small-angle reflections are due to smectic layers (arrow 1), and wide-angle reflections are due to the molecular arrangement of mesogenic groups (the director) within the smectic layers (arrow 2).

temperature in the SmX\* and SmC\* phases.  $\theta_E$  remains at about 10° in the temperature region of the SmA phase at 90 °C, and it also remains at several degrees even in the isotropic phase at 130 °C. In the same manner as the sample length  $L_E$ ,  $\theta_E$  also changes in the reverse order during the cooling process. Namely,  $\theta_E$ , which is several degrees in the isotropic phase, increases with decreasing temperature, and then it becomes about 24° at room temperature. It should be pointed out that this value almost agrees with that of the initial state. The monodomain SmC\* elastomer possesses the ability to restore its shape spontaneously. Additionally it has to be emphasized that the shape memory effect of the monodomain SmC\* is a biaxial deformation process due to the spontaneous shear deformation. The shape change of the elastomer film seems to be closely associated with the local symmetry of the corresponding liquid-crystalline phase. To analyze whether macroscopic shape changes directly correlate with molecular re-alignment processes, X-ray investigations are carried out. The X-ray patterns at various temperatures are shown in Figure 5, where the small-angle reflections are due to smectic layers (arrow 1) while the azimuthal intensity maxima at wide-angle reflections indicate molecular



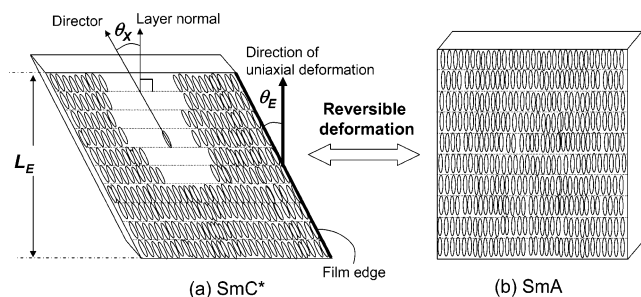


**Figure 6.** Schematic model for shape change of elastomer film with molecular realignment. The macroscopic symmetry defined by the shape of the  $\text{SmC}^*$  elastomer film corresponds to the microscopically local symmetry due to the molecular alignment of the liquid-crystalline phase of  $\text{SmC}^*$ .

orientation of mesogenic groups (the director) within the smectic layers (arrow 2).

Figure 5a shows the X-ray pattern of the monodomain  $\text{SmC}^*$  elastomer observed at room temperature (25 °C). While the layer reflection located near the meridian indicates a uniform alignment of smectic layers in the tilted smectic phase at room temperature, reflection at a wide angle indicates that the mesogenic groups are aligned uniformly in the direction inclined as  $\theta_x$  with respect to the layer normal. By comparison of both X-ray patterns of parts a and b of Figure 5, we recognize that the location of wide-angle reflection rotates clockwise with increasing temperature, while the layer reflection remains near meridian. Namely, the mesogens inclined with respect to the layer normal in Figure 5a are rearranged in the direction parallel to the layer normal in Figure 5b, although the direction of the layer normal is almost independent of temperature. Since the smectic–isotropic phase transformation occurs with further increasing temperature, only halos are observed at 130 °C (Figure 5c).

In the cooling process shown in parts c–e of Figure 5, the reverse change of the molecular alignment is confirmed. As shown in Figure 5d, the layer reflection appears at the meridian and the molecular reflection simultaneously emerges at a wide angle on the equator during the isotropic to  $\text{SmA}$  phase transition. With decreasing temperature the location of the wide-angle reflection rotates anticlockwise, and then it reverts to the original position at room temperature (Figure 5e). Since the residual tilted order originating from cross links commands mesogens to tilt in the direction of the original orientation, they accordingly tilt in the same direction during the  $\text{SmA}$ – $\text{SmC}^*$  phase transformation. As the internal shear stress originating from cross links induces the macroscopically uniform molecular tilting,<sup>33</sup> the monodomain  $\text{SmC}^*$  elastomer is to hold the memory of its original alignment.

According to the correspondence of the sample observation (Figure 3) to the X-ray scattering pattern (Figure 5), we are able to schematize the relationship between the shape change of the elastomer film and the molecular rearrangement during  $\text{SmC}^*$ – $\text{SmA}$  phase transformation in Figure 6 where the shape of elastomer film is closely associated with the local symmetry of the liquid-crystalline phase. Subsequently, we would like to analyze quantitatively the X-ray patterns at various temperatures for further investigation on the behavior of the phase transformations. Figure 7 shows the temperature dependence of the molecular tilt angle  $\theta_x$ , which is defined as the angle between the director and the layer normal (see Figure 5a and Figure 6). The value

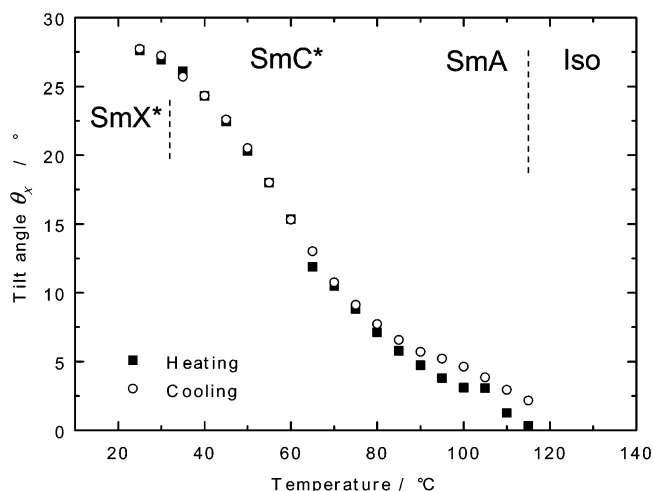


**Figure 7.** Temperature dependence of molecular tilt angle  $\theta_x$ , which is defined as an angle between the director and the layer normal in the X-ray scattering pattern.

of  $\theta_x$ , which is about 25° at room temperature (25 °C), rapidly decreases with increasing temperature in the  $\text{SmX}^*$  and  $\text{SmC}^*$  phases. While the gradient of the dispersion curve becomes less above about 80 °C due to  $T_{\text{CA}}$ ,  $\theta_x$  remains at several degrees even in the temperature region of the  $\text{SmA}$  phase in the same manner as the tilt angle of elastomer film  $\theta_E$ . Since the residual  $\text{SmC}^*$  order is fixed by cross linking of the polymer backbone, the rearrangement for the suitable molecular alignments is disturbed at the phase transformation from  $\text{SmC}^*$  to  $\text{SmA}$ . It must be noted that the experimental results on cooling almost perfectly agrees with those on heating (Figure 7).

It has to be emphasized that the tilt angle of the elastomer film  $\theta_E$  approximately agrees with the molecular tilt angle  $\theta_x$  characterized in the X-ray patterns. Namely, the macroscopic symmetry defined by the shape of the  $\text{SmC}^*$  elastomer film corresponds directly with the microscopic local symmetry due to the molecular alignment of the liquid-crystalline phase of  $\text{SmC}^*$ , as depicted in the schematic model of Figure 6. We can conclude that cross linking between polymer backbones under mechanical shear field produces the monodomain  $\text{SmC}^*$  elastomer in which a memory of the biaxially molecular alignment of the  $\text{SmC}^*$  state is perpetuated even after exposure to the isotropic state. Consequently, the monodomain  $\text{SmC}^*$  elastomer exhibits the biaxial shape memory effect in its macroscopic feature. Moreover, it is expected that interesting physical properties, such as ferroelectricity,<sup>20</sup> pyroelectricity,<sup>21</sup> and second harmonic generation<sup>22</sup> due to the macroscopic  $C_2$  symmetry of the unwound  $\text{SmC}^*$  state, are also memorized in the elastomer. These will be described in a forthcoming paper.

To consider more details of the mechanism which controls molecular reorientation and macroscopic shape change in the monodomain  $\text{SmC}^*$  elastomer,  $\theta_E$  is plotted as a function of  $\theta_x$  in Figure 8. Here, the values of  $\theta_E$  in the isotropic phase at 130 °C are also plotted on the ordinate. Nonlinearity is apparently recognized in the relationship between  $\theta_x$  and  $\theta_E$ , despite an expected linear relation due to the supposed direct coupling between them in our simple model illustrated in Figure 6. Let us tentatively explain the emergence of the nonlinearity, based on a hypothesis that not mesogens but the topology of cross linkers have an

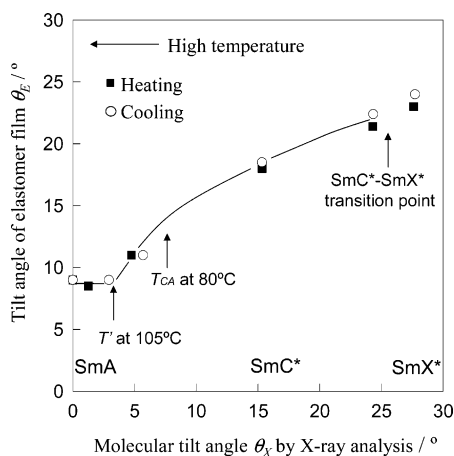


**Figure 8.** Relationship between the molecular tilt angle  $\theta_X$  determined by the X-ray scattering pattern and the tilt angle of elastomer film  $\theta_E$  in a monodomain SmC\* elastomer.

ability to change the elastomer shape. Here, we need to investigate the details of the tilting behavior around the SmC\*–SmA transformation in the same manner as reported in a previous paper.<sup>25</sup> As already mentioned in the Experimental Section, the SmC\*–SmA transformation temperature  $T_{CA}$  has been determined at 80 °C on the basis of the temperature dependence of molecular tilt angle calculated from the layer thickness of the uniaxially deformed elastomer. On the other hand, we have simultaneously noticed that the smectic layers apparently tilt with respect to director just above the SmC\*–SmA transformation temperature  $T_{CA}$ , because the in-plane chevron structure observed in the SmC\* phase remains.<sup>25,34</sup> With further increasing temperature, the layer tilt angle decreases to zero at 105 °C, which is tentatively designated as  $T'$ . Both  $T_{CA}$  at 80 °C and  $T'$  at 105 °C are marked in Figure 8 on the basis of the temperature dependence of  $\theta_X$  in Figure 7.

In Figure 8,  $\theta_E$  increases with increasing  $\theta_X$  not only in the temperature range of the SmC\* and SmX\* phases but also in the part of the SmA region below  $T'$ , while it remains almost constant above  $T'$ . The slope of the dispersion curve is relatively steep in the temperature region from  $T'$  at 105 °C probably to  $T_{CA}$  at 80 °C, where an internal shear stress is introduced by the topology of cross links and retains the layer tilting despite the constant layer thickness. This implies that in fact not mesogens but cross linkers dominate the tilting behavior here, because the tilt angle of mesogens should be constant. Since the polymer networks forming the sample shape are fixed by the cross linkers, the change of tilt of cross linkers brings about a shape change in this temperature region. Moreover, we can say that the SmC\* state is, at least partly, induced by the internal shear stress in the temperature region between  $T'$  and  $T_{CA}$ . On the other hand, the slope becomes gradual in the SmC\* temperature region less than  $T_{CA}$ . Since mesogens, whose numbers are eight times larger than those of cross linkers, dominate the tilting behavior in this temperature region, the layer tilting is accompanied with a decrease of layer thickness. Because of the intralayer fluidity in the smectic C phase, the tilting of mesogens does not be effect the shape-change with varying  $\theta_E$  in the SmC\* phase. To discuss the nonlinear relationship between molecular reorientation and macroscopic shape change as a whole is beyond the scope of this paper. In the meantime, we proceed to make further observations on the deformation behavior and

hope to elucidate a number of mechanistic questions. We will show experimental details to confirm our hypothesis soon.

## Conclusion

We have shown that a monodomain chiral smectic C elastomer exhibits a biaxial shape memory effect, demonstrating its spontaneous and reversible deformation on heating and cooling where successive phase transitions took place. Not only shrinkage (elongation) due to the smectic–isotropic (isotropic–smectic) transition but also spontaneous shear deformation associated with molecular tilting in the temperature range of the smectic phases was observed. In addition, the reverse change of the molecular alignment was also confirmed by the X-ray observation during the heating and cooling process. The agreement between the sample observation and the X-ray analysis revealed that the macroscopic symmetry defined by the shape of the SmC\* elastomer film was closely associated with the microscopic local symmetry due to the liquid-crystalline phase. Because cross-linking under mechanical shear field perpetuated the memory of the molecular alignment at the SmC\* state, the monodomain SmC\* elastomer exhibited a biaxial shape memory effect in the macroscopic feature of the film. In addition, we tentatively explained the nonlinearity in the relationship between  $\theta_E$  due to the elastomer shape and  $\theta_X$  estimated by X-ray observations on the basis of a hypothesis that not mesogens but the topology of cross linkers have an ability to change the elastomer shape.

**Acknowledgment.** This work was supported by Deutsche Forschungsgemeinschaft, SFB 428. In addition, the Tokyo group was supported by the “Academic Frontier” Project for Private Universities (2001–2005) and the Grant-in Aid for Scientific Research (No. 17550169): matching fund subsidy from the Ministry of Education, Culture, Sports, Science and Technology (MEXT).

## References and Notes

- (1) Finkelmann, H.; Kock, H. J.; Rehage, G. *Makromol. Chem., Rapid Commun.* **1981**, 2, 317.
- (2) Zentel, R.; Reckert, G. *Makromol. Chem.* **1986**, 187, 1915.
- (3) Mitchell, G. R.; Devis, F. J.; Ashman, A. *Polymer* **1987**, 28, 639.
- (4) Brand, H. R.; Finkelmann, H. *Handbook of Liquid Crystals*; Demus, D., Goodby, J., Gray, G. W., Spiess, H.-W., Vill, V., Eds.; Wiley-VCH: Weinheim, 1998; Vol. 3, pp 277–302.
- (5) Zentel, R. *Angew. Chem. Adv. Mater.* **1989**, 101, 1437.
- (6) Devis, F. J. *J. Mater. Chem.* **1993**, 3, 551.
- (7) Warner, M.; Terentjev, E. M. *Liquid Crystal Elastomers*; Clarendon Press: Oxford, 2003; pp 1–7 and 93–106.
- (8) Küpfer, J.; Finkelmann, H. *Makromol. Chem., Rapid Commun.* **1991**, 12, 717.
- (9) de Gennes, P. G. *C. R. Acad. Sci.* **1997**, 324, 343.
- (10) Thomsen, D. L., III; Keller, P.; Naciri, J.; Pink, R.; Jeon, H.; Shenoy, D.; Ranta, B. R. *Macromolecules* **2001**, 34, 5868.
- (11) (a) Finkelmann, H.; Wermter, H. *ACS Abstr.* **2000**, 219, 189. (b) Wermter, H.; Finkelmann, H. *e-Polymers* **2001**, no. 013 ([http://www.e-polymers.org/papers/finkelmann\\_210801.pdf](http://www.e-polymers.org/papers/finkelmann_210801.pdf)).
- (12) Tajbakhsh, A. R.; Terentjev, E. M. *Eur. Phys. J. E.* **2001**, 6, 181.
- (13) Nishikawa, E.; Finkelmann, H.; Brand, H. R. *Macromol. Rapid Commun.* **1997**, 18, 65.
- (14) Zanna, J. J.; Stein, P.; Marty, J. D.; Mauzac, M.; Martinoty, P. *Macromolecules* **2002**, 35, 5459.
- (15) Assfalg, N.; Finkelmann, H. *Macromol. Chem. Phys.* **2001**, 202, 794.
- (16) Nishikawa, E.; Yamamoto, J.; Yokoyama, H.; Finkelmann, H. *Macromol. Rapid Commun.* **2004**, 25, 611.
- (17) Adams, J. M.; Warner, M. *Phys. Rev. E* **2005**, 71, 021708.

- (18) Meyer, R. B. *Mol. Cryst. Liq. Cryst.* **1977**, *40*, 33.
- (19) Zentel, R. *Liq. Cryst.* **1988**, *3*, 531.
- (20) Brehmer, M.; Zentel, R.; Wagenblast, G.; Siemensmeyer, K. *Macromol. Chem. Phys.* **1994**, *195*, 1891.
- (21) Lehmann, W.; Leister, N.; Hartmann, L.; Geschke, D.; Kremer, F.; Stein, P.; Finkelmann, H. *Mol. Cryst. Liq. Cryst.* **1999**, *328*, 437.
- (22) Benné, I.; Semmler, K.; Finkelmann, H. *Macromol. Rapid Commun.* **1994**, *15*, 295.
- (23) Eckert, T.; Finkelmann, H. Keck, M.; Lehmann, W.; Kremer, F. *Macromol. Rapid Commun.* **1996**, *17*, 767.
- (24) Lehmann, W.; Skupin, H.; Tolksdorf, C.; Gebhard, E.; Zentel, R. Krüger, P.; Löcshe, M.; Kremer, F. *Nature* **2001**, *410*, 447.
- (25) Hiraoka, K.; Uematsu, Y.; Stein, P.; Finkelmann, H. *Macromol. Chem. Phys.* **2002**, *203*, 2205.
- (26) Hiraoka, K.; Stein, P.; Finkelmann, H. *Macromol. Chem. Phys.* **2004**, *205*, 48.
- (27) Rousseau, I. A.; Mather, P. T. *J. Am. Chem. Soc.* **2003**, *125*, 15300.
- (28) Terentjev, E. M.; Warner, M. *J. Phys. II* **1994**, *4*, 849.
- (29) Warner, M.; Terentjev, E. M. *Liquid Crystal Elastomers*; Clarendon Press: Oxford, 2003; pp 350–356.
- (30) (a) Semmler, K.; Finkelmann, H. *Polym. Adv. Technol.* **1994**, *5*, 231. (b) Semmler, K.; Finkelmann, H. *Macromol. Chem. Phys.* **1995**, *196*, 3197.
- (31) Hiraoka, K.; Finkelmann, H. *Macromol. Rapid Commun.* **2001**, *22*, 456.
- (32) Martinot-Lagarde, Ph. *J. Phys. C* **1976**, *3*, 129.
- (33) Noirez, L.; Lapp, A. *Phys. Rev. Lett.* **1997**, *78*, 70.
- (34) Hiraoka, K.; Finkelmann, H. Unpublished results.

MA050642C